

COAGULATION AND CRYSTALLIZATION OF SILICATES IN PROTOPLANETARY DISKS: A C2D SPITZER/IRS SURVEY

Olofsson, J.¹, Augereau, J.-C.¹, Monin, J.-L.¹ and the c2d IRS team

Abstract. Silicates are observed in almost every place where dust can survive: in the interstellar medium (ISM), in the Earth mantle, in comets and it is now common knowledge that there are also present in circumstellar disks around young stars. The ISM sub-micron sized silicates are highly amorphous (>99%), while the silicate Mg-rich crystallinity fraction can reach 60% in comets like Hale-Bopp in the Solar System. The silicates have to be exposed to high temperatures to crystallize, and their presence in long-period comets suggests that dust has been heavily processed and transported in the disk. Statistical studies of planet forming disks are keys on understanding if these processes are generic and can occur in other protoplanetary systems.

As part of the Cores to Disks (c2d) Legacy Program, we obtained more than a hundred of Spitzer/IRS spectra of T Tauri stars, in the spectral range 5-35 μm , where many crystalline features are present. We find that most of these objects ($\sim 70\%$) show silicate emission features, either attributed to amorphous or crystalline grains. Studying the 10 μm feature, we find that grain growth has occurred and their quasi-systematic presence in the disks upper layers indicate ongoing turbulent vertical mixing. We will also show that crystalline dust grains are present in the outer/deeper cold regions of the disk, with typical temperatures of about 100 K, which suggests efficient radial transport mechanisms. Overall, our study shows that vertical and radial transport seem to be generic dynamical processes in disks, challenging theoretical disk evolution and planet formation models.

1 Introduction

Silicates dust grains in the interstellar medium (ISM) are known to be largely amorphous ($\sim 99\%$) and with a typical sub-micronic grain size (e.g. Gail et al. 1998). On the other side, studies of comets in the Solar System present high crystallinity fraction. For example, Wooden et al. (1999) showed that 60% of the silicate grains in comet Hale-Bopp are crystalline grains, while Jupiter Family comets have a slightly lower crystallinity fraction (of about 35%), but still high compared to the ISM. This difference can be explained considering a radial dependance of the mineralogy inside the disk. Therefore, it is meaningful to consider silicate crystalline grains as being tracers of the history of the circumstellar disk. During this stage of evolution, silicate grains are expected to be heavily processed, by coagulation, fragmentation and crystallization, caused by stellar radiation, thermal agitation, collisions, for instance.

The first observations of silicates in circumstellar disks have been obtained from the ground. Because of the atmosphere, only the 10 μm feature, produced mainly by amorphous grains, could be observed. Thanks to ISO satellite, mid to far-IR spectroscopy of disks around Herbig Ae/Be stars (hereafter, HAeBe) that are more massive than the Sun, could be achieved. Acke & van der Acker (2004), showed that 52% of HAeBe stars present the 10 μm feature, and 23% of them show the 11.3 μm feature, which is associated to forsterite, an Mg-rich crystalline silicate. Spitzer satellite then became available and several surveys were led (e.g. Furlan et al. 2006, Kessler-Silacci et al. 2006), but also detailed studies of individual objects, like the borderline brown dwarf (hereafter, BD) BD2 from Merín et al. (2007) or the BD in the Taurus cloud from Bouy et al. (2008).

We present in the following, some results from the c2d Spitzer Legacy Program “From Molecular Clouds to Planets” (Evans et al. 2003). This work is the continuation of a series of papers, studying the grains, PAHs and the gas in the inner disk regions around young stellar objects. In Sec. 2, we first present general results on the apparition of crystalline features, then in Sec. 3, we study the relations between the different crystalline features and finally, in Sec. 4 we address the question of the typical grain sizes in our sample.

¹ Laboratoire d’Astrophysique de Grenoble, CNRS/UJF UMR 5571, 414 rue de la Piscine, B.P. 53, F-38041 Grenoble

2 Crystallinity in circumstellar disks

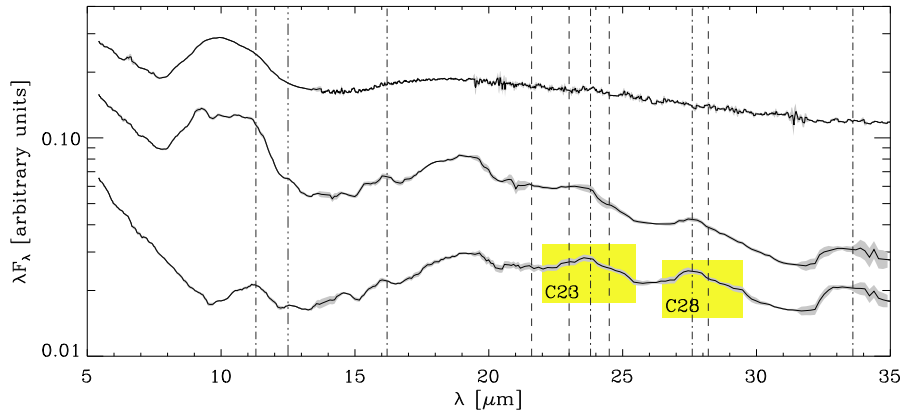


Fig. 1. From bottom to top, Spitzer/IRS spectra of ISO-ChaII 54, SSTc2d J033036.0+303024 and AS 205, in arbitrary units of λF_λ . The vertical lines show the peak positions of the enstatite (dashed lines) and forsterite (dot-dashed lines) crystalline features we attempt to identify in every spectrum of our 110 star sample. The two boxes correspond to the C23 and C28 crystalline complexes.

2.1 IRS observations and source sample

We present in this study the infrared spectra of disks around 110 young stellar objects, obtained as part of the c2d Legacy Program. The spectra were obtained using the InfraRed Spectrograph (IRS) instrument onboard the Spitzer Space Telescope. The sample is mainly composed of Class II objects, even if 39 of them have no classification in the literature, but show clear amorphous silicate features in emission. The source list contains 110 stars, distributed among 6 major clouds: Perseus (16 objects), Taurus (9), Chamaleon (23), Ophiuchus (26), Lupus (16), Serpens (16) plus 4 isolated stars. Out of these 110 stars, 60 are young solar analogs (TTauri stars, hereafter TTs), 9 are HAeBe and 1 is a BD. The 40 other young objects have no known classification. Fig.1 shows the different kind of spectra we have in our sample, from amorphous to very crystalline (e.g. ISO-ChaII 54).

2.2 Crystalline species

In many spectra, broad 10 and 20 μm features can be easily identified and are attributed to amorphous silicate grains. But narrower features due to crystalline grains can also be identified. In this study we consider features arising from Mg-rich silicates, enstatite (pyroxene group) and forsterite (olivine group). The example spectrum of ISO-ChaII 54 displayed in Fig.1 shows that the 23.0, 24.5 μm enstatite and the 23.8 μm forsterite features can be blended into one single complex. The same happens to the 27.6 μm forsterite feature with the 28.2 μm enstatite feature. In the following we will treat these features as two complexes, independent of the actual crystals responsible for their emission, and will refer to them as the C23 and C28 complexes.

2.3 Fraction of disks showing silicates features

We develop an IDL routine that determines the characteristics of the crystalline features, mainly, the peak positions, peak fluxes and line fluxes. Only 6 objects out of the 110 spectra we study do not show any amorphous or crystalline silicates features. What comes out first from this analysis is that silicate crystallization is not a marginal phenomenon in Class II circumstellar disks, since both the C23 and C28 complexes are present at rates higher than 50%. The amorphous 10 μm feature on the other hand has an apparition frequency of about $\sim 65\%$, which is consistent with the analysis on HAeBe stars from Acke & van der Acker (2004). The question of the localisation of these silicates is addressed in Sec. 3.

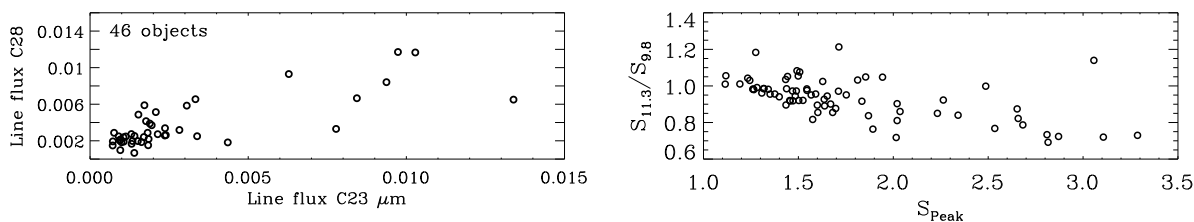


Fig. 2. *Left panel:* Normalized line fluxes correlation between the C23 and C28 complexes. *Right panel:* Correlation between shape and strength of the amorphous $10\ \mu\text{m}$ feature. Large grains ($a \sim 1.0\ \mu\text{m}$) are located on the left side of the plot.

3 Localisation of silicate grains

3.1 Relationship between the $10\ \mu\text{m}$ feature and the crystallinity

We evaluate in the following the relationship between the $10\ \mu\text{m}$ amorphous feature and the crystallinity probed by features arising at wavelengths larger than $20\ \mu\text{m}$, mainly the two complexes C23 and C28 and the forsterite feature at $33.6\ \mu\text{m}$. To achieve this, we search for correlations between the energy contained in the various features. To get rid of possible distance and/or brightness effect, we normalise the line flux by the mean value of the estimated continuum multiplied by the central wavelength. To quantify the presence of a correlation, we compute a Kendall τ test, which returns a τ value (between -1. and +1.) and a probability P that there is no correlation. A $\tau = 1$ means that the correlation is perfect, while a τ value of -1 means that it is a perfect anti-correlation. For the $10\ \mu\text{m}$ feature and the C23 complex, we find $\tau = 0.08$ and $P = 0.43$ that the two *line fluxes* are not correlated. For the $10\ \mu\text{m}$ feature and the C28 complex; we obtain $\tau = -0.028$ and $P = 0.8$ (no correlation). Regarding the $10\ \mu\text{m}$ feature and the $33.6\ \mu\text{m}$ feature we compute a τ value of 0.11 and $P = 0.44$, that they are not correlated. To verify this first tendency, we compute correlation coefficients on the *apparition frequency* of the corresponding features. For the $10\ \mu\text{m}$ and the C23, we have $\tau = 0.046$ with $P = 0.49$. With the C28, we obtain $\tau = 0.094$ and $P = 0.159$. Finally, between the 10 and $33.6\ \mu\text{m}$ features, we have $\tau = -0.021$ and a probability $P = 0.753$ that the presence of these two features are not correlated. Overall this suggests that the crystalline features observed at wavelengths larger than $20\ \mu\text{m}$ and the amorphous $10\ \mu\text{m}$ feature do arise from independent grain populations. In addition to this, we investigate the effect of the shape of the $10\ \mu\text{m}$ feature, which is related to the grain size (see Sec. 4), as a function of the presence of one of the two complexes C23 or C28. We find that there is no relation between the grain size of grains emitting at $10\ \mu\text{m}$ and the presence of the two complexes. This basically means that the growth of the grains emitting at $10\ \mu\text{m}$ is not linked to the degree of crystallinity of the grains emitting at wavelengths larger than $20\ \mu\text{m}$.

3.2 Relationship between crystalline features

Grains probed by emission at $10\ \mu\text{m}$ and emission at $\lambda > 20\ \mu\text{m}$ do come from independent dust population, but is it the same for crystalline grains that emit at large wavelengths? We compute correlation coefficients, the same way as explained above (Sec. 2), for C23, C28 and the $33.6\ \mu\text{m}$ feature. Regarding the line fluxes emitted by the two complexes, C23 and C28, we obtain $\tau = 0.53$ and $P = 2.4 \times 10^{-7}$ (see left panel of Fig. 2), for the C23 complex and the $33.6\ \mu\text{m}$ feature, we have $\tau = 0.54$ and $P = 1.5 \times 10^{-4}$ showing that there is correlation. For the C28 complex and the $33.6\ \mu\text{m}$ feature, we obtain $\tau = 0.58$ and $P = 1.8 \times 10^{-4}$, confirming the fact that crystalline features emitting at wavelengths larger than $20\ \mu\text{m}$ are correlated to each others, and thus are probably probing the same dust population.

4 Deriving typical grain sizes

4.1 The amorphous $10\ \mu\text{m}$ feature

The amorphous $10\ \mu\text{m}$ feature is present at a rate higher than 65% in our sample. Bouwman et al. (2001), van Boekel et al. (2003) or Kessler-Silacci et al. (2006) have shown that detailed study of this feature can provide

a lot of information on the dust characteristics and in particular on the typical size of the emitting grains. To perform this analysis, we use the same computation method as the one described in Kessler-Silacci et al. (2006), i.e. building two indexes at 9.8 and 11.3 μm from a normalized spectrum, and plotting their ratio as a function of the strength of the feature. We find that there is an anti-correlation, with $\tau = -0.44$ and a probability $P = 5.96 \times 10^{-8}$ that there is no correlation, as shown in the right panel of Fig. 2. This correlation can be interpreted as larger grains producing flatter features. Using theoretical opacities, we show that the bulk of the points is located in the place where the typical grain size is micronic. This means that for grains emitting the 10 μm feature, grain growth has taken place.

4.2 The C23 complex

In the following we attempt to find a similar correlation for the C23 complex. We use the same computation method as before and build two indexes, at 23 and 24 μm . The correlation coefficient between the ratio of these two indexes and the strength of the C23 complex is $\tau = -0.56$ with a probability below the IDL simple precision that there is no correlation. Also, using theoretical opacities, we find that grain growth has occurred for grains that produce the C23 complex.

5 Conclusion

Compared to the silicate mineralogy in the ISM, we show that strong modifications occurred inside a majority of circumstellar disks. Mainly, grain growth has taken place, for all grains that are probed by Spitzer/IRS spectra. Secondly, crystallinity is not a marginal phenomenon in disks compared to the ISM, the apparition frequency of crystalline silicates is about $\sim 50\%$ in young circumstellar disks. This means that dust is subject to a strong and efficient process that modify its lattice structure.

The study of the shape versus the strength of different features not only showed that grain growth has occurred, we also learned something about the hydrodynamical state of the disk. In a simple case where turbulence is not present in the disk, we can expect to see a strong settling of intermediate-sized grains ($\sim 1.0 \mu\text{m}$) toward the midplane. The fact that we can see large grains in the optically thin layers of the disk means that turbulence is still very active and sufficient to vertically mix the grains.

Finally, we find that grains emitting at 10 μm and grains emitting at wavelengths larger than 20 μm are arising from independent dust populations. Considering a simple Wien's law, the first population is close to the star, and rather warm ($T \sim 300\text{-}600\text{ K}$) while the second one is much colder (typically 100 K). The fact that this cold dust component shows many crystalline features is intriguing: we indeed expect the crystalline grains to form by thermal annealing, requiring temperatures larger than 800 K, while we see crystalline grains at $T \sim 100\text{ K}$. This indicates that a radial transportation mechanism is very active inside the disk.

References

- Acke, B. & van den Ancker, M. E. 2004, *A&A*, 426, 151
 Bouwman, J., Meeus, G., de Koter, A., et al. 2001, *A&A*, 375, 950
 Bouy, H., Huelamo, N., Pinte, C., et al. 2008, *ArXiv e-prints*, 803
 Evans, II, N. J., Allen, L. E., Blake, G. A., et al. 2003,
 Furlan, E., Hartmann, L., Calvet, N., et al. 2006, *ApJS*, 165, 568
 Gail, H.-P. 2004, *A&A*, 413, 571
 Kessler-Silacci, J., Augereau, J.-C., Dullemond, C. P., et al. 2006, *ApJ*, 639, 275 *PASP*, 115, 965
 Merín, B., Augereau, J.-C., van Dishoeck, E. F., et al. 2007, *ApJ*, 661, 361
 van Boekel, R., Waters, L. B. F. M., Dominik, C., et al. 2003, *A&A*, 400, L21
 Wooden, D. H., Harker, D. E., Woodward, C. E., et al. 1999, *ApJ*, 517, 1034